EFFECTS OF TUNNEL CROSS-SECTION SHAPE ON THE STRESS DISTRIBUTION AROUND THE TUNNEL IN SANDY SOILS

Zelin ZHOU[1], Hirokazu AKAGI[2], Alireza AFSHANI[3], Shengwei ZHU[3]

[1]Non-Member of JSCE, Dept. of Civil and Environmental Eng., Waseda University
(3-4-1 Okubo, Shinjuku-ku, Tokyo 169-8555, Japan)
E-mail: zhou0914@akane.waseda.jp
[2]Fellow Member of JSCE, Professor, Dept. of Civil and Environmental Eng., Waseda University
(3-4-1 Okubo, Shinjuku-ku, Tokyo 169-8555, Japan)
E-mail: akagi@waseda.jp
[3]Member of JSCE, Technical Department Part 2, Obayashi Corporation
(2-15-2 Kounan, Minato-ku, Tokyo 108-8502, Japan)
E-mail: afshani@moegi.waseda.jp
[3]Non-Member of JSCE, Assistant, Dept. of Civil and Environmental Eng., Waseda University
(3-4-1 Okubo, Shinjuku-ku, Tokyo 169-8555, Japan)
E-mail: suonigou@aoni.waseda.jp

Rectangular, or quasi-rectangular tunnels have become popular recently due to their advantages of reducing the excavation volume, effectively utilizing the underground space, and smaller impact on the existing structure in proximity. To clarify the difference of the stresses distribution between the quasi-rectangular tunnel and the circular tunnel in sandy soils, an experimental study using the aluminum bars and three tunnel models with cross-section shapes of circle, quasi-rectangle with long-axis in the horizontal direction, and quasi-rectangle with long-axis in the vertical direction are conducted in this research. Discrete element method (DEM) is used to obtain the stress distribution around the three tunnels with different cross-section shapes. The numerical study is verified by the displacement fields observed in the experimental study. A parametric study of the width to height ratio of the tunnel cross-section is performed. By combining the displacement fields obtained from the experiment test, and the stress distribution around the tunnel obtained from the numerical study, the effect of cross-section shape of tunnel in sandy soils is investigated.

Key Words : *Quasi-rectangular tunnels, Discrete element method, Stress distribution around tunnel*

1. INTRODUCTION

When constructing an subway tunnel with a shield machine, the tail gap between the soil and lining induced by overcutting will allow surrounding soil particles to move towards the lining. Such convergence of the soils will cause a decrease of the earth pressure acting on the crown of tunnel lining and form a loosening zone in adjoining soils, reflecting the soil arching effect. It is observed from field measurements that the vertical pressures acting on the tunnel lining are reduced by 20-60% of the overburden earth pressure in sandy soils[1)].

Peck[2)] showed that the surface settlement distribution induced by ground loss of tunnel construction could be considered as a Gaussian curve. Wu[3)] proposed an analytical solution to establish a relationship between ground loss and arching effect in tunneling. However, only circular shape tunnel was considered in their reseraches.

Recently, the construction of rectangular or quasi-rectangular tunnels have increased due to their advantages of reducing excavation and efficient use of the underground space[4)]. For the circular tunnel, many researchers have conducted a large amount of theoretical research[3)], model tests[5)], and numerical analyses[6)] on investigating the soil arching effect induced by tunnel excavation. However, not so many researches on the stress distribution of quasi-rectangular tunnels have been performed so far.

Due to the irregular shape of a quasi-rectangular tunnel, the movement of surrounding soils and ground settlement will appear differently from those of circular tunnels, which may influence the formation of loosening zone and stress redistribution around the tunnel[7)]. Therefore, it is crutial to investigate the influence of the tunnel shapes on the stress distribution around the tunnels.

To clarify the tunnel shapes effect, an experimental study using aluminum bars and models of three tunnels with cross-section of circle, quasi-rectangle with long-axis in the horizontal direction, and quasi-rectangle with long-axis in the vertical direction are conducted in this research.

A simplified two-dimensional plane strain DEM (discrete element method) model with the same dimension as the experiment is established, and the stress distribution around the three different shapes of tunnels are examined. Finally, a parametric study of the rectangular tunnels with various width to height ratio are performed to further investigate the tunnel shape effects, and the reduction of stress in soil around the tunnels are compared with Terzaghi's lossening pressure to check the validaity of the numerical model. By analyzing the amount of soil displacement in the experiment and stress distribution from numerical DEM model, it was found that for a same amount of volume loss, a larger width to height ratio of the tunnel tends to have a smaller vertical stress reduction on the tunnel crown and a larger horizontal stress reduction at the spring line of the tunnel.

2. EXPERIMENTAL STUDY

(1) Apparatus of the experimental model

As a first part of this study, in order to examine the effect of various cross-section shapes of tunnel on the displacement distribution and stress release in soil around tunnel after shield machine pass, a shield tunneling modeling device was prepared and then series of experimental tests were performed. In this part, details of physical model as well as shield tunneling modeling device are introduced in details and then experiment cases are explained, and finally the results are presented.

The physical model consists of two wood columns, stacks of aluminum bars, and a shield tunnel modelling device, as shown in **Fig. 1**. The wood columns are located on both sides with a spacing of 338 mm. The shield tunnel modelling device is placed in between and the lower middle of the two wood columns. The aluminum bars are stacked horizontally in parallel around the tunnel model. The overburden height of the tunnel model is 310 mm.

The shield tunnel modeling device consists of a metal axis with screw threads, two cones made of polymer, and a rotating handle as shown in **Fig. 2**. It is used to simulate the convergence of soil towards the lining after the shield machine has passed. By rotating the handle, cones are separated and aluminum stacks moves gradually toward the cone center (tunnel center). By rotating an angle of 120°, the cones are separated by 4 mm, and aluminum bars move towards the tunnel model by 1 mm. The handle is rotated at a rate of 120° per min, and stops for each rotating in order to take a photo of the state of aluminum bars. By rotating of handle, aluminum bars can move radially by maximum amount of 9 mm. Because of followed procedure, the experiment is referred to quasi-static conditions. Then the photos are analyzed by particle image flow (PIV) program to obtain the displacement fields of the aluminum bars.

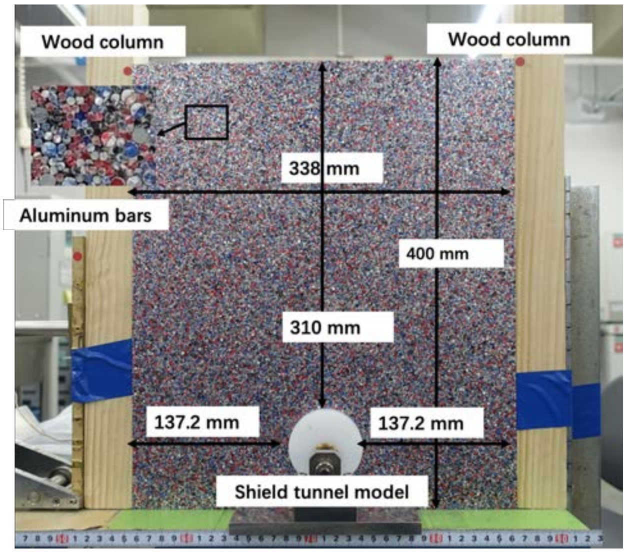

Fig. 1 Front view of the experimental apparatus.

As shown in **Fig. 3**, there are three types of tunnel models with the same cross-section contraction patterns adopted in this study. The invert of the tunnel models is fixed. The circular tunnel model has a maximum radius of 31.8 mm. The quasi-rectangular tunnel model with a long axis in the horizontal direction has a maximum cross-section of 66 mm × 55 mm and a width to height ratio of b/a = 6/5. The quasi-rectangular tunnel model with a long axis in the vertical direction has a maximum cross-section of 55 mm × 66 mm and a width to height ratio of b/a = 5/6.

The maximum inward aluminum bars movement of the three tunnel models is 9 mm. The design of the quasi-rectangular tunnel models are based on the cross-section of a real metro tunnels with long axis in horizontal direction and another tunnel with long axis in vertical direction in Tokyo metropolitan area. All three models have identical cross-sectional area.

Tunnel volume loss is defined as the ratio of soil loss volume to total excavation soil volume per unit tunnel length, V_l, which can be expressed as:

$$V_l = \frac{\pi(D^2 - D'^2)}{\pi D^2} \tag{1}$$

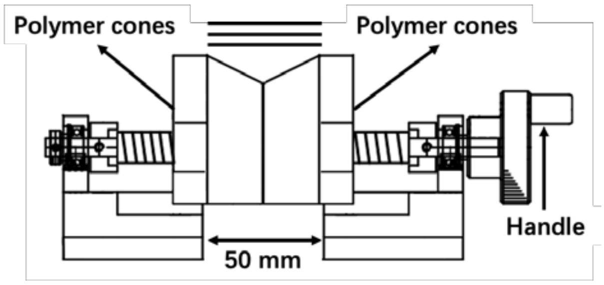

Fig. 2 Shield tunnel modelling device.

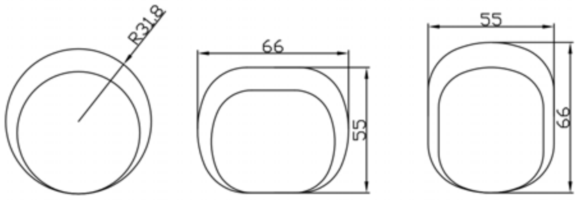

Fig. 3 Cross-section of the circular tunnel model, quasi-rectangular tunnel model with a long axis in the horizontal direction and quasi-rectangular tunnel model with a long axis in the vertical direction.

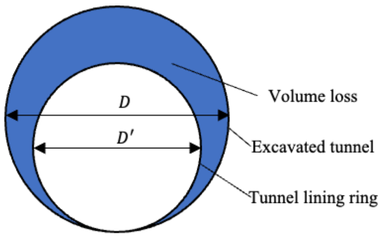

Fig. 4 Volume loss of the circular tunnel.

where D is the excavated diameter of tunnel; D' is the external diameter of tunnel lining ring, as shown in **Fig. 4**. In this study, V_l is considered as the ratio of the reduced cross-sectional area to the initial cross-sectional area of the tunnel model.

(2) Material properties of aluminum bars

The material properties of aluminum bars are shown in Table 1. The aluminum bars used in the experiment are a mixture of 1.6 mm and 3.0 mm in diameter and are in the ratio of 2:1 in mass, which are determined by the particle size distribution curve of standard Toyoura sand[8]. The length of the aluminum bars are 50 mm, and the unit weight of the aluminum bars mass is 20.4 KN/m^3. The internal friction angle of the aluminum bars mass is 25° which is obtained from the laboratory tilt test, as shown in Fig. 5. The coefficient of restitution is the ratio of relative velocity after collision to relative velocity before collision of the material. In this paper, the coefficient of restitution, Young's modulus and Poisson's ratio of the aluminum bars are decided by the material properties of aluminum.

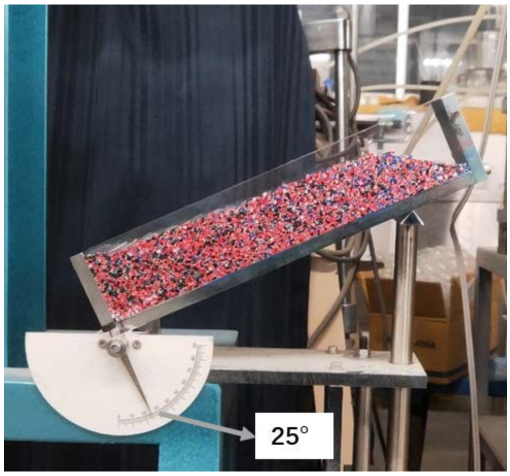

Fig. 5 Laboratory tilt test of the aluminum bars

Table 1 Material properties of the aluminium bars.

Parameters	Values
Young's modulus (GPa)	71
Poisson's ratio	0.34
Coefficient of restitution	0.1
Internal friction angle (°)	25

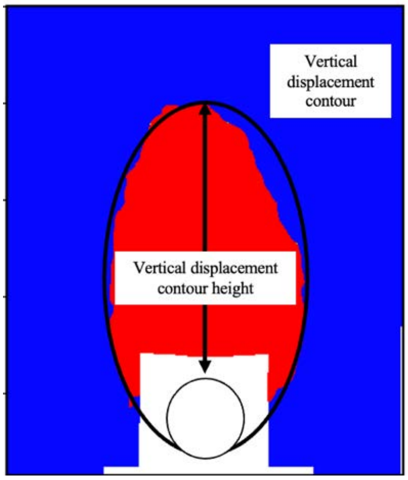

Fig. 6 Vertical displacement contour of the circular tunnel.

(3) Results

In order to compare the extent of loosening zone area under arching effect in three tunnel cases, vertical displacement are obtained by partice image flow (PIV) program. The vertical displacement contour is generated by setting the vertical displacement at the value of 1.8 and 2.7 mm, which are 20% and 30% of the maximum inward aluminum bars movement (9 mm). The vertical displacement contour height is the distance from the crown of the tunnel to the top of the displacement contour. **Fig. 6** shows an example of the vertical displacement contour height obtained from

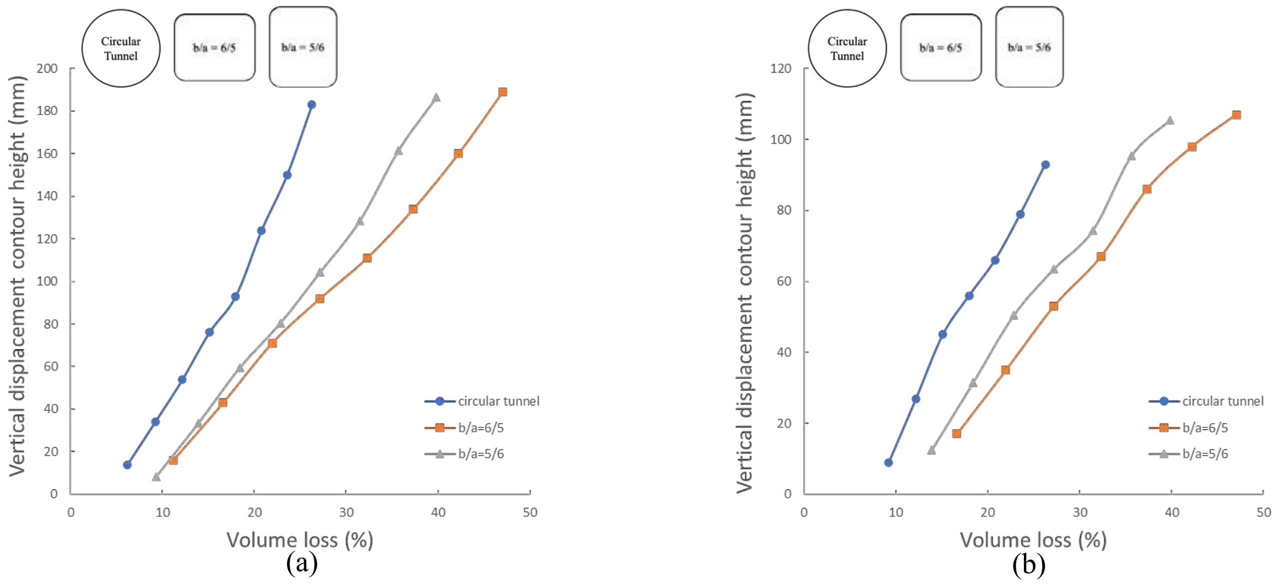

Fig. 7 Evolution of the vertical displacement contour height for three tunnel shapes in the case of the vertical displacement of the aluminum bars is 1.8 mm (a), and 2.7 mm (b).

the DEM program for circular tunnel. The red area shows soil loosening zone generated by the effect of radial particle movements toward tunnel center. The white zone is the location of the tunnel. Due to the rectangular shape and larger size of the mesh, the white zone is in rectangular shape and occupy a larger area than the tunnel.

Fig. 7 shows the the vertical displacement contour height evolution in the case of vertical displacement of 1.8 mm (a), and 2.7 mm (b) for the three tunnels with different cross-sectional shapes. The abscissa represents the volume loss of tunnel by percentage for each 1 mm inward movement of the aluminum bars, and the ordinate shows the values of vertical displacement contour height.

In **Fig. 7**, for both cases of (a) and (b) and for identical amount of volume loss, the circular tunnel has a larger vertical displacement contour height than the other two quasi-rectangular tunnels. The quasi-rectangular tunnel with width to height ratio of 6/5 has the smallest displacement contour height. This phenomenon indicates that a larger loosening zone is formed in the case of circular tunnel.

3. NUMERICAL STUDY

The discrete element method (DEM) was developed by Cundall and Stack[9)] as a method for analyzing the motion of discontinuous particles such as rock and sand.

In the experimental study, stress distribution around the tunnel model unable to be obtained. To obtain the stress around tunnels and to investigate the deformation mechanisms of granular materials, a two-dimensional numerical model is built by using DEM code on the basis of the linear spring-dashpot contact model[10].

(1) DEM model for the circular and quasi-rectangular tunnel

The DEM model has the same dimension as the experimental model. The particle mass is a mixture of large and small particles with diameter of 1.6 mm and 3 mm. There are in total 5278 large particles and 37344 small particles used in the DEM model, which are decided by the mass ratio of the aluminum bars mass.

The cross-section of tunnel models are the same as those used in the experimental study, as shown in **Fig. 3**. When conducting the numerical simulation, the cross-sectional area of the tunnel model is reduced proportionally. The maximum soil inward movement of the tunnel is 10 mm. For every 1 mm inward soil movement, the aluminum bars around the tunnel will converge and move towards the tunnel ring, in order to simulate the experiment procedure.

(2) Mechanical parameters of the DEM model

Based on the linear spring-dashpot contact model[10)], for the two-dimensional model, the normal stiffness coefficient between particles k_{np}, and the normal stiffness coefficient between particles and the wall k_{nw} are:

$$k_{np} = \frac{R_1 \cdot E^*}{R_1 + R_2} \tag{2a}$$

$$k_{nw} = 2 \cdot E^* \tag{2b}$$

where R_1 is the smaller radius of the aluminum bars, R_2 is the larger radius of the aluminum bars, and E^*

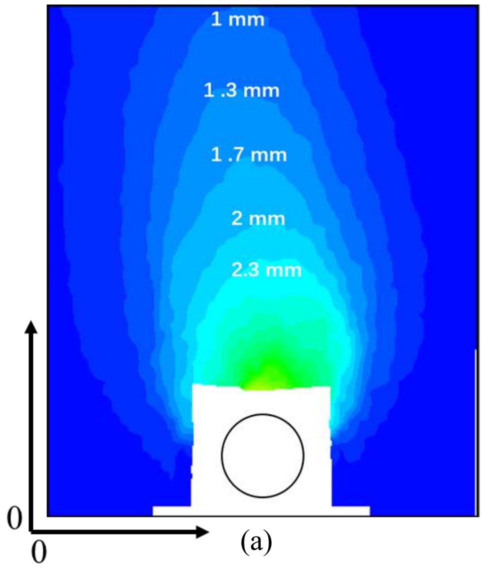

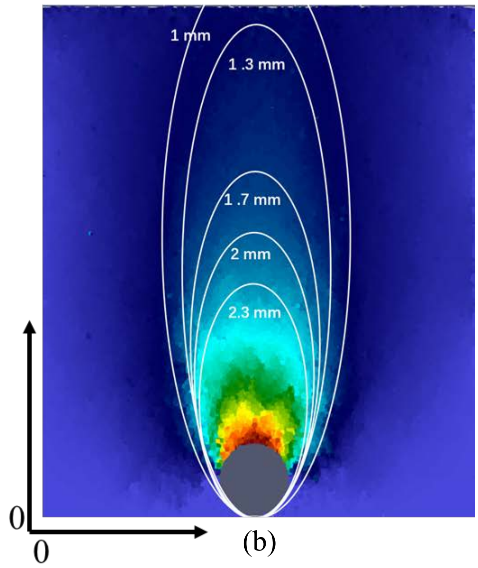

Fig. 8 Vertical displacement fields of the aluminum bars experiment (a), and DEM model (b).

is the effective modulus of the contact defined by Mindlin[12)], which can be obtained by followed equation:

$$\frac{1}{E^*} = \frac{1-v_1}{E_1} + \frac{1-v_2}{E_2} \tag{3}$$

where E_1, E_2 are Young's modulus and v_1, v_2 are the Poisson's ratio of the contacting particles.

Based on the elastic solid mechanics analysis of Mindlin (1949), the shear stiffness k_s can be obtained by:

$$\frac{k_s}{k_n} = \frac{1-v}{1-0.5v} \tag{4}$$

where k_n is the normal stiffness, and v is the Poisson's'ratio of the contacting materials.

It is proven by Lommen (2014) et al. that E^* in the range of 1×10^5– 1×10^{11} Pa has no significant influence on the mechanical behavior of the simulated particles. Due to this fact and to save the calculation time, the value of normal contact stiffness coefficient is set at 1×10^4 N/m. Additionally, the Young's modulus of the wall is assumed equal to that of the aluminum bars.

The friction coefficient of the contact is decided by the internal friction angle of the aluminum bars, and the damping ratio ζ of the contact is decided by the coefficient of restitution e of the aluminum bars, which is:

$$\zeta = -\frac{lne}{\sqrt{\pi^2 + ln^2 e}} \tag{5}$$

By substituting the material properties of aluminum bars into **Eq. 2a, 2b, 3, 4 and 5**, the mechnical parameters of the DEM model are obtained and listed in **Table 2**.

Table 2 Mechnical parameters of the DEM model.

Mechnical Parameters	**Values**
Normal stiffness coefficient of the contact between particles, k_{np}, (N/m)	1×10^4
Shear stiffness coefficient of the contact between particles, k_{sp} (N/m)	0.8×10^4
Normal stiffness coefficient of the contact between wall and particles, k_{nw} (N/m)	3×10^4
Shear stiffness coefficient of the contact between the wall and particles, k_{sw} (N/m)	2.4×10^4
Friction coefficient of the contact, μ	0.5
Damping ratio, ζ	0.6

(3) Verification and validation of the numerical simulation

Fig. 8 shows the vertical displacement fields of the DEM and experimental model when the maximum inward radial movement of the circular tunnel is 9 mm. From this figure, it can be seen that for the range of vertical displacement from 1.5 to 5 mm, the results of DEM and experiment considerably match with each other.

Fig. 9 (a), (c) and **(e)** show the variation of loosening height by volume loss in the case of 1.8 mm vertical displacement contour for three tunnel shapes. Similarly, **Fig. 9** **(b), (d)** and **(f)** show the variation of loosening height by volume loss in the case of 2.7 mm vertical displacement contour for three tunnel shapes.

For the circular tunnel and the quasi-rectangular tunnel with width to height ratio of b/a = 6/5, the DEM results match the experiment results well, while in the case of quasi-rectangular tunnel with width to height ratio of b/a = 5/6, the experiment results dem-

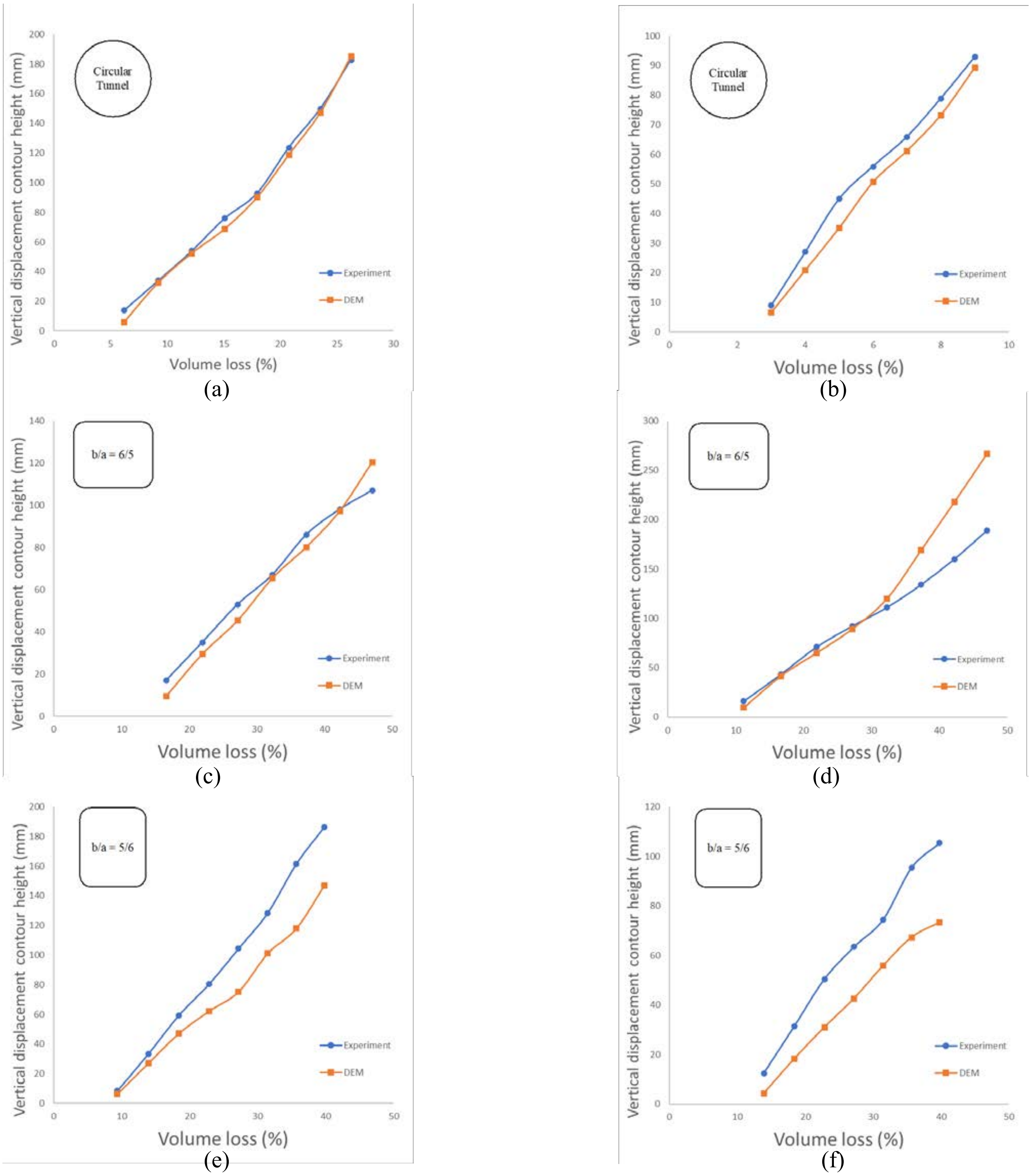

Fig. 9 Variation of loosening height by volume loss in the case of 1.8 mm vertical displacement contour for three tunnel shapes, (a), (c) and (e). Variation of loosening height by volume loss in the case of 2.7 mm vertical displacement contour for three tunnel shapes, (b), (d) and (f).

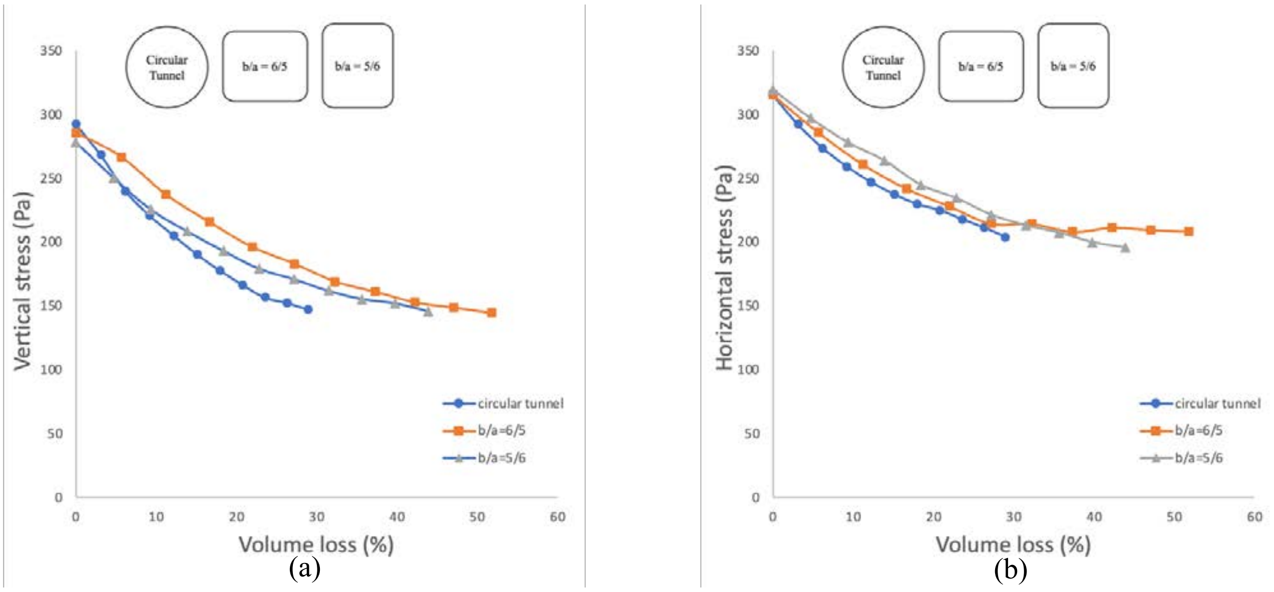

Fig. 10 Comparison of variation of vertical stress on the crown of the tunnel by volume loss among three tunnels with different cross-section shapes, (a). Comparison of variation of horizontal stress at the spring line of the tunnel by volume loss among three tunnels with different cross-section shapes, (b).

onstrates higher lossening heights. By employing the current DEM parameters, fair degree of matching can be seen between numerical DEM results and aluminum bars experiment output.

(4) Comparison of the stress distribution among three tunnels with different shapes

Fig. 10 (a) shows the variation of vertical stress on the crown of the tunnels by increase of volume loss for three tunnels with different cross-section shapes. For a same amount of volume loss, the circular tunnel experiences the most significant reduction of vertical stress compared with the other two tunnel, and the quasi-rectangular tunnel with width to height ratio of b/a = 6/5 has the least significant reduction of vertical stress.

Fig. 10 (b) shows the variation of horizontal stress on the left and right spring line of the tunnel (the results of the left and right spring line of the tunnel are almost the same) by increase of volume loss for three tunnels with different cross-section shapes. As shown in this figure, for a same amout of volume loss, the circular tunnel has the largest reduction of horizontal stress compared with the other two tunnel shapes, and the quasi-rectangular tunnel with width to height ratio of b/a = 5/6 has the smallest reduction of horizontal stress. When the value of volume loss reaches 27%, the horizontal stress of tunnel with width to height ratio of b/a = 6/5 almost remain unchanged, and the the horizontal stress of tunnel with width to height ratio of b/a =5/6 decreases sharply in comparison with case of b/a = 6/5.

In **Fig. 10 (a)** and **(b)**, it is shown that the decrease of vertical stress at tunnel crown and horizontal stress at tunnel spring lines tends to level off when the volume loss exceed a certain, in this case, around 30%, which coincides with the analytical solution by Wu[3].

4. SENSITIVITY ANALYSIS

(1) Comparison of the stress distribution among rectangular tunnels with various width to height ratio

In the engineering practice, a rectangular shield tunnel may be designed to have a vertical section for single track, or a horizontal section for double or multiple tracks, which causes the width to height ratio varying in a certain range. In this study, with the DEM model, the stress distribution around tunnels when width-to-height ratio from 3/4 to 5/3 is investigated.

To further investigate the influence of tunnel shapes on the stress distribution around the tunnel, a parametric study of the rectangular tunnels with a same height and various width to height ratio (b/a = 3/4, 1, 4/3, and 5/3) are performed are performed. The height of the rectangular tunnel is taken to be 60 mm, and the mechanical parameters of the DEM model are the same as the previous numerical study.

Fig. 11 shows the variation of vertical stress on the crown of the tunnel as the volume loss increases for the tunnels with different width to height ratio of b/a = 3/4, 1, 4/3, 5/3. It can be observed that the tunnel with a smaller width to height ratio have a larger decrease in vertical stress.

Fig. 12 shows the variation of horizontal stress at the left and right spring line by changes of volume loss for the tunnels with different width to height ratio. It indicates that the tunnel with a larger width to height ratio tends to have a larger decrease in horizontal stress. However, compared with the case of vertical stress, the difference in horizontal stress distribution among tunnels with different width to height ratio is relatively small.

Fig. 13 shows the variations of K (ratio of horizontal stress to vertical stress = σ_h/σ_v) by volume loss at the tunnel spring line for different shapes of tunnels. It can be seen that the K ratio is almost unchanged after volume loss of 10% among all tunnel cases.

(2) Comparison between the Terzaghi's loosening pressure and numerical results

Terzaghi method[11] is the most acknowledged solution to estimate the loosening earth pressure on deep buried tunnels. For deep buried tunnels, the pressure on the crown of the tunnel can be obtained by:

$$\sigma_v = \frac{\gamma B_1}{K\, tan\phi} \cdot \left(1 - e^{-K\, tan\phi \cdot D_1/B_1}\right) + \gamma D_2 e^{-K\, tan\phi \cdot D_1/B_1} \qquad (6)$$

where σ_v is the loosening earth pressure on the tunnel crown, K is the ratio of horizontal earth pressure to vertical earth pressure, ϕ is the internal friction angle of soils, γ is the unit weight of soil, c is cohesion of soil, D_1 is the height of the loosening zone, D_2 is the distance from the top of the loosening zone to the ground surface and B_1 is the yielding strip of tunnel. Terzaghi proposed that the yielding strip B_1 was:

$$B_1 = R_o \cdot \cot\left(\frac{\pi/4 + \emptyset/2}{2}\right) \qquad (7)$$

which is much wider than that observed in model tests (Lee 2006). In this part, B_1 is taken to be .uivalent to initial with of the rectangular tunnel. The values of the other parameters are shown in **Table 3**, which obtained based on the physical and material properties of the aluminum rods.

By applying all the parameters of **Table 3** into **Eq. 6**, Terzaghi's loosening earth pressure is obtained and compared with the vertical stress obtained by DEM model when volume loss of the tunnel is 31% (Based on Wun's study[3], the decrease of loosening pressure on the crown of the tunnel is relatively small when the volume loss is larger than 31%), as shown in **Fig. 14**. The abscissa represents the vertical stress reduction versus initial vertical stress ($\frac{\sigma_{v1}-\sigma_{vo}}{\sigma_{vo}}$%), and the ordinate is the width to height ratio of the rectangular tunnels. From **Fig. 14**, it can be seen that in the case of the tunnel width to height ratio are b/a = 3/4 and b/a = 5/3, the loosening earth pressure of the DEM model is almost the same as the Terzaghi's loosening earth pressure, while in the case of the tunnel width to height ratio are b/a = 1 and b/a = 4/3, the loosening earth pressure of DEM model is larger than Terzaghi's loosening earth pressure.

Nevertheless, both Terzaghi' solution and DEM simulation results show that a tunnel with smaller width to height ratio has a larger loosening pressure on the tunnel crown.

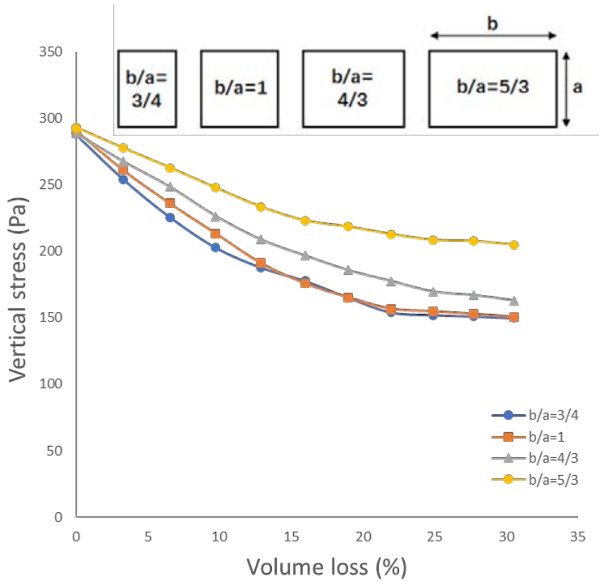

Fig. 11 Comparison of vertical stress on the crown of the tunnel among three tunnels with width to height ratio.

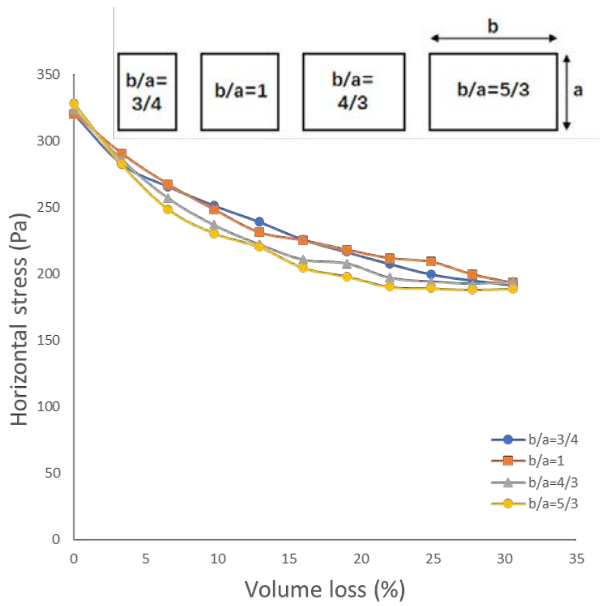

Fig. 12 Comparison of horizontal stress at the left and right spring line of the tunnel among three tunnels with width to height ratio.

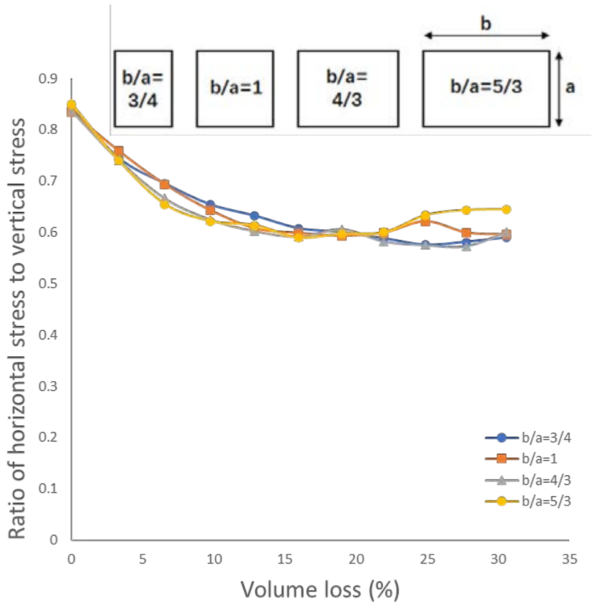

Fig. 13 Comparison of ratio of horizontal stress to vertical stress *K* at the left and right spring line of the tunnel among three tunnels with width to height ratio.

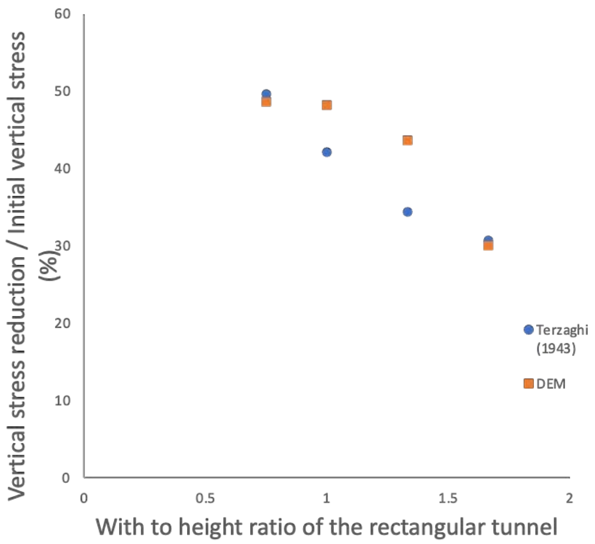

Fig. 14 Comparison of the vertical stress reduction on the crown of the tunnel between Terzaghi's solution and DEM simulation.

Table 3 Parameters of the Terzaghi's loosening earth pressure

Parameters	Values
B_1 (m)	71
Unit weight of soil, γ (N/m3)	969.3
Ratio of horizontal earth pressure to vertical earth pressure, K	0.83
height of the loosening zone, D_1 (m)	0.09
distance from the top of the loosening zone to the ground surface, D_2 (m)	0.19
Internal friction angle (°)	25

5. CONCLUSIONS

The shape effects of tunnel in sandy soils is studied both experimentally and numerically. The relationship between the stress around the tunnel and volume loss of tunneling was established based on the results obtained by the experimental and numerical model. Variations of loosening heights with volume loss for three types of cross-sectional dimension ratio were performed. The main conclusions are summarized as follows:

1) In the experimental study, the shape effect of tunnels is carried out by comparing the loosening heights of the three different shapes of tunnels. The values of loosening heights among three tunnel cases are: circular tunnel > quasi-rectangular tunnel of b/a = 5/6 > quasi-rectangular tunnel of b/a = 6/5.
2) The verification of DEM model is conducted by using the loosening heights observed in the experiment test. In the case of vertical displacement contour of 1.8 and 2.7 mm, the DEM computed results agrees fairly with the results observed in the experimental study.
3) In the numerical study, the stress distribution around the three tunnels with different cross-section shapes are obtained. The numerical results show that the relation of the vertical stress reduction on the crown of the tunnel among three tunnel cases are: circular tunnel > quasi-rectangular tunnel with long axis in the vertical direction > quasi-rectangular tunnel with long axis in the horizontal direction. In the case of the horizontal stress reduction at the spring line of the tunnel among three tunnel cases are: circular tunnel > quasi-rectangular tunnel with long axis in the horizontal direction > quasi-rectangular tunnel with long axis in the vertical direction.
4) The sensitivity analysis shows the width to height ratio of the tunnel will affect the extent of arching effect. The results show that a larger width to height ratio of the tunnel will lead to a smaller vertical stress reduction at the tunnel crown and a larger horizontal stress reduction at the spring line of the tunnel. In addition, the amount of vertical stress reduction ratio is fairly close to that obtained by Terzaghi method.

ACKNOWLEDGMENT: The author would like to appreciate Professor Hirokazu Akaki, Dr. Alireza Afshani Mehrabad, and Mr. Shengwei Zhu for their helpful advice and great supports in this work. He also want to thank to Mr. Benjamin and Mr. Esaki for their great help in preparing the experiment and DEM code. A special thank to his family and lovely fiancée who supports him financially and emotionally in preparing this paper.

REFERENCES

1) Inokuma, A., Ishimura, T. : Earth pressure acting on shield driven tunnels in soft ground. *Underground Construction in Soft Ground*, Rotterdam, The Netherlands. pp. 221–224, 1995.
2) Peck, R.B. : Deep excavations and tunnelling in soft ground. State-of-the-art-report. *In: Proceedings of 7th International Conference of Soil Mechanics and Foundation Engineering*, ISSMGE, Mexico City, Mexican. pp. 225–281, 1969.
3) Wu, J., Liao, S.M., Liu, M.B. : An analytical solution for the arching effect induced by ground loss of tunneling in sand. *Tunn. Undergr. Space Technol*. 83, pp. 175–186, 2019.
4) Zeng GS, Wang HN, Jiang MJ. : Analytical study of ground responses induced by the excavation of quasirectangular tunnels at shallow depths. *Int J Numer Anal Methods Geomech*. 1–24, 2019.
5) Lee, C.-J., Chiang, K.-H., Kuo, C.-M. : Ground movement and tunnel stability when tunneling in sandy ground. *J. Chin. Inst. Eng*. 27 (7), 1021–1032, 2004.
6) Jiang, M.J., Yin, Z.Y. : Analysis of stress redistribution in soil and earth pressure on tunnel lining using the discrete element method. *Tunnel Underground Space Technol*. 32, 251–259, 2012.
7) Liu, X., Liu, Z., Yuan, Y., & Zhu, Y. : Quasi-Rectangular Shield Tunneling Technology in the Ningbo Rail Transit Project. *In High Tech Concrete: Where Technology and Engineering Meet* pp. 2765-2773. Springer, Cham, 2018.
8) Shiratori, K., Yamashita, Y. and Adachi, Y. : Deposition and subsequent release of Na-kaolinite particles by adjusting pH in the column packed with Toyoura sand, *Colloid. Surface. A*., 306(1-3), 137-141, 2007.
9) Cundall, PA, Strack, ODL. : A discrete numerical model for granular assemblies. *Geotechnique*. 29(1):47–65, 1979.
10) ITASCA. : *PFC2D Online Manual, Table of Contents – Theory and Background –, Section 1: General Formulation*, 2002.
11) Terzaghi, K. : Theoretical Soil Mechanics. *John Wiley & Sons*, NewYork, 1943.
12) Mindlin, R. : Compliance of elastic bodies in contact. *J. Appl. Mech*. 16, No. 3, 259–268, 1949.